CORROSION SCIENCE AND TECHNOLOGY, Vol.14, No.6(2015), pp.253~260 pISSN: 1598-6462 / eISSN: 2288-6524
DOI: http://dx.doi.org/10.14773/cst.2015.14.6.253

Can the Point Defect Model Explain the Influence of Temperature and Anion Size on Pitting of Stainless Steels

Daniel J. Blackwood†

Department of Materials Science & Engineering, National University of Singapore,1 Engineering Drive 2, Singapore 117576
(Received July 22, 2015; Revised November 03, 2015; Accepted November 03, 2015)

The pitting behaviours of 304L and 316L stainless steels were investigated at 3 °C to 90 °C in 1 M solutions of NaCl, NaBr and NaI by potentiodynamic polarization. The temperature dependences of the pitting potential varied according to the anion, being near linear in bromide but exponential in chloride. As a result, at low temperatures grades 304L and 316L steel are most susceptible to pitting by bromide ions, while at high temperatures both stainless steels were more susceptible to pitting by small chloride anions than the larger bromide and iodide. Thus, increasing temperature appears to favour attack by smaller anions. This paper will attempt to rationalise both of the above findings in terms of the point defect model. Initial findings are that qualitatively this approach can be reasonably successful, but not at the quantitative level, possibly due to insufficient data on the mechanical properties of thin passive films.

Keywords : *stainless steel, pitting corrosion, anion size*

1. Introduction

The pitting potential (E_p) of stainless steels varies with both the nature of the aggressive ion and temperature. Further it has been shown that E_p declines exponentially with increasing temperature in chloride but only linearly in bromide[1-3], which leads to a cross over temperature below which bromide is more aggressive than chloride, but above which the order is reversed. That is increasing temperature seems to favour pitting by smaller anions. The E_p identified from potentiodynamic polarisation is best interpreted as the potential above which nucleated pits can propagate to achieve stable growth so it is more characteristic of pit growth processes rather than passivity breakdown[4-6]. However, although pit growth is likely dominated by the transport of ions into or out of the pit[6], it is not clear how this process can explain the temperature dependence of the order of aggressiveness of the halide ions. For example, although the specific conductance (predominately due to ion transport) of a moderately conductive halide solution (e.g. 1 M) varies almost linearly with temperature, the slope is virtually independent of anion size (ca. 2 % K^{-1}) and thus would not lead to a cross-over temperature for the relative aggressiveness of bromide and chloride.

The point defect model has been developed by Macdonald to explain the pit initiation[7,8]. Although it is recognized that the pitting potential determined from the potentiodynamic polarization experiments is unlikely to be the critical breakdown potential of the passive film used in the Point Defect Model (PDM), the two parameters are clearly related to one another, i.e. if the breakdown potential increases than E_p can be expected to also increase. Hence if the PDM predicts a temperature dependence for the relative order of the halide induced critical breakdown potentials, then this could also explain the relative behaviour of the E_p's.

According to the point defect model the initial event in passivity breakdown is absorption of aggressive ions into surface oxygen vacancies[7]. This contains three energetic steps that are related to the size of the aggressive ion:

(i) energy required to physically increase the size of the surface oxygen vacancy (ΔG_{Exp});
(ii) dehydration energy of the aggressive species (ΔG_{Dehyd});
(iii) energy required to insert dehydrated aggressive species into the expanded vacancy (ΔG_{Insert}).

Macdonald has shown that the energetic of this initial step depends on the size of the surface oxygen vacancy and thus argued that this can explain why the aggressiveness of a halide ion depends on its size[7]. For example the fact that chloride is generally more aggressive to ferrous alloys but bromide is to titanium alloys can be ex-

† Corresponding author: msedjb@nus.edu.sg

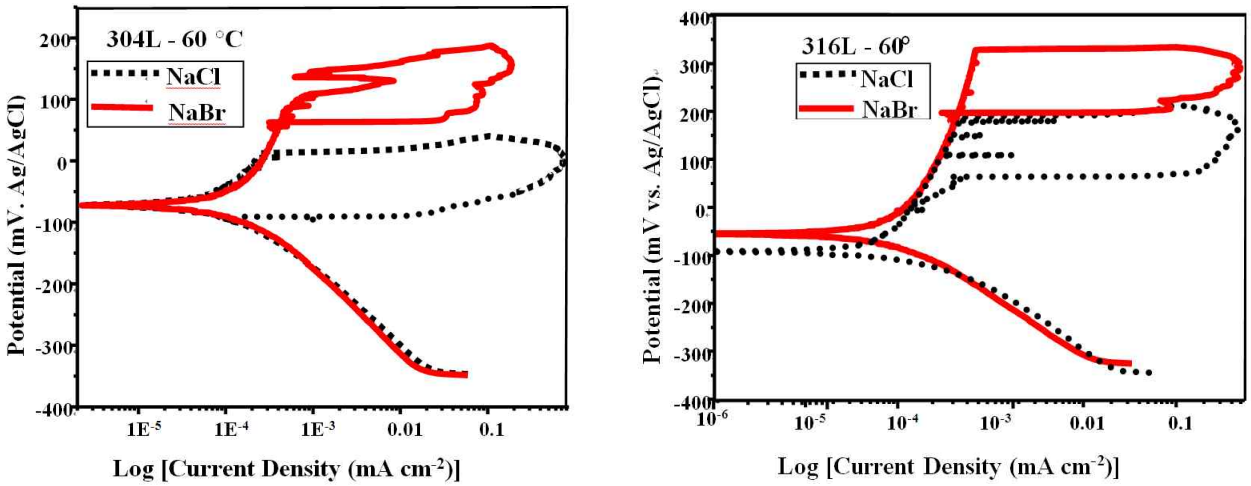

Fig. 1. Typical potentiodynamic curves for 304L (left) and 316L (right) stainless steel in 1M NaCl (black dotted) and 1M NaBr (red solid) at 60 ℃.

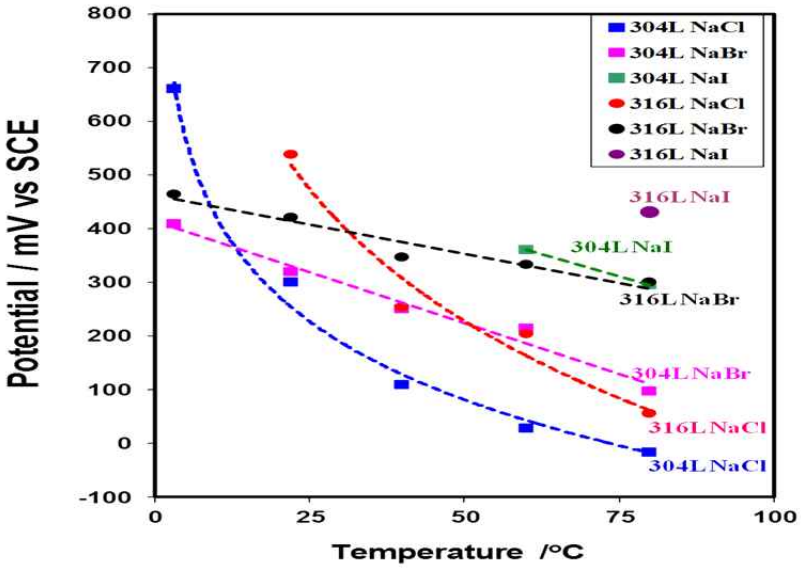

Fig. 2. Influence of temperature on the pitting potentials of 304L and 316L stainless steels in 1M NaX.

plained if the oxygen vacancies are larger in the latter alloys; unfortunately data on the size of oxygen vacancies in most passive is lacking so it is not possible to validate this hypothesis.

In this present paper the temperature dependencies of the three energetic steps involved in the absorption of aggressive ions into surface oxygen vacancies will be evaluated to determine if the point defect model can explain the influence of temperature on relative aggressiveness of halogen ions.

2. Experimental Procedure

Both 304L (UNS S30403) and 316L (UNS S31603) specimens were cut from 3 mm thick plates into rectangles measuring 50 x 10 mm. In accordance with ASTM G61 all samples were wet-grind with 320-grit SiC paper, and then with 600-grit SiC paper until coarse scratches were removed followed by ultrasonic cleaning in deionised water and ethanol for 10 minutes[9]. Prior to assembly, samples were degreased for 5 minutes in detergent and water, rinsed thoroughly in distilled water and then dried.

The electrochemical experiments were conducted in a conventional three-electrode cell. The counter electrode was a graphite rod and the reference electrode was a Ag/AgCl (3.5 M KCl) and all potentials quoted in this paper are versus this system. The temperature range investigated was 3 ℃ to 90 ℃ and electrolyte solution used was 1M sodium halide (chloride, bromide or iodide) prepared by dissolving reagent grade chemicals in de-ionized

water.

Pitting potentials were determined via potentiodynamic polarization according to ASTM G61[9]. The solution was deoxygenated by bubbling nitrogen throughput the experiment and the specimen was immersed for about 1 hour before recording the open-circuit potential and initiating polarization curve; controlled by Gamry Instruments E-Corrosion Software. The starting potential was 350 mV vs. Ag/AgCl and the scan rate was 10 mV min^{1}. Once the current density reached 0.1 mA cm^{-2} the scan direction was reversed until the hysteresis loop closed. Each potentiodynamic curve was repeated at least 3 times.

3. Results and Discussion

Fig. 1 shows typical potentiodynamic curves for 316L stainless steel in 1M NaCl and 1M NaBr at 60 ℃, show that at this temperature pitting occurs easier in chloride than bromide. Fig. 2 shows plots of the temperature dependence pitting potentials of 304L and 316L in the 1M sodium halide solutions. It can be seen that the temperature dependence of both alloys is a much stronger in chloride than in bromide and this is more pronounced in 316L than in 304L. This is in agreement with the work of Truman[3] where in chloride solutions the E_p's of the two stainless steels were found fall almost exponentially with temperature, with 316L having the steeper gradient, as well as that of Munoz *et al*[2]. who reported a near linear relationships between the pitting potential and solution temperature for superaustenitic stainless steels in concentrated bromide environments.

As a result of the different temperature dependences of the E_p in the halide solutions cross over temperature below which chloride is more aggressive than bromide, but above which bromide is the more aggressive. Fig. 2 suggest that the cross-over temperatures are about 22 ℃ and 30 ℃ for 304L and 316L respectively. In NaI solutions pitting only occurred at high temperature, so insufficient data was obtained to determine temperature dependence of the pitting potential in this media, suffice to say it was the least aggressive halide at all temperatures investigated.

According to the point defect model the first step in the pitting mechanism is the adsorption of an aggressive ion (X) into a surface oxygen vacancy and this has previously been identified as the step that is dependent on anion size[7];

$$V_O^{\bullet\bullet} + X^- \cdot nH_2O \rightarrow X_O^{\bullet} + nH_2O \quad (1)$$

Where $V_O^{\bullet\bullet}$ is an oxygen vacancy of radius r_o and $X_O^{\bullet}$ is a halide ion located at an oxygen vacancy site now of radius r_{Xo}. This is followed by migration of cation vacancies through the passive film and their condensation at the metal/oxide interface, preventing the oxide from continuing to grow and thus causing a pit to initiate as dissolution continues at the oxide / solution interface.

Intuitively one may think that an increase in temperature will cause an expansion of the vacancy size making pitting by larger ions more favorable, which is opposite to the experimental evidence in Fig. 2 that shows Cl^- becomes more aggressive than Br^- at higher temperatures. However, this initial intuitive idea of an expansion in the oxygen vacancy size can easily be shown to be incorrect. Given that the coefficients of thermal expansion of metal oxides are less than 10^{-5} K^{-1}, then over the temperature range presently investigated the volume change will << 1 %. Therefore the oxygen vacancy size can be assumed to be independent of temperature, an assumption that becomes even more valid when one considers that thermodynamics dictates that the number of defects increases with temperature[10].

As mentioned in the introduction, Reaction (1) can be broken down into three energetic steps, anion dehydration; oxygen vacancy expansion and insertion of the dehydrated anion, all of which will be influenced by temperature. The approach below is mainly based on that adopted by Macdonald to explain the influence of anion size on the breakdown potential[7].

3.1 Dehydration energy

$$V_O^{\bullet\bullet} + X^- \bullet nH_2O \xrightarrow{\Delta G_{Dehydr}} X_O^{\bullet} + nH_2O \quad (2)$$

Table 1. Sizes and hydration energies of the various halide ions as measured by Schmid *et al*[11]

Anion	Size (Å)	ΔG (kJ mol^{-1})	ΔH (kJ mol^{-1})	ΔS (J mol^{-1} K^{-1})
F-	1.36	-501	-539	-127
Cl-	1.81	-373	-392	-65
Br-	1.95	-346	-361	-49
I-	2.16	-311	-321	-31

Table 1 shows the hydration energies of the various halide ions as measured by Schmid *et al*[11]. along with the radii of the dehydrated anions as reported by Conway[12]. Since an ion's dehydration energy is simply the negative its hydration energy, it is clear that the smaller halides are harder to dehydrate, thus this term favours pitting by larger ions; the large dehydration energy of fluoride ions has been proposed to be the reason why these halide causes general corrosion rather than localised corrosion of a number of titanium and aluminium alloys[13].

Furthermore, as ΔS_{Dehyd} is positive increasing the temperature will make pitting more favourable but there should be no change in the order of aggressiveness of the ions. However, as the entropy terms are more than 10^3 times smaller than their enthalpy counterparts the ΔG_{Dehydr}'s will decline by less than 10 kJ mol^{-1} over the temperature range investigated and there will be no change in their order with respect to anion size.

Fig. 3 shows plots of ΔG_{Dehydr} versus the reciprocal of the anion radius at 273K and 373K, which can be seen to linear passing through (or at least very close to) the origin. Hence of ΔG_{Dehydr} can be expressed as a function of temperature and anion radius:

$$\Delta G_{Dehydr} = \frac{(a - bT)}{r} \quad kJ\ mol^{-1} \tag{3}$$

where a and b are constants.

Finally, as pointed out by Macdonald[7], it needs to be noted Reaction (2) should also take into account the energies for dehydration of the oxygen vacancy and rehydration of the inserted anion

$$V_O^{\bullet\bullet}\cdot mH_2O + X^-\cdot nH_2O \rightarrow X_O^{\bullet}\cdot pH_2O + (m+n-p)H_2O \tag{4}$$

Unfortunately, values for these two additional parameters do not exist, but it can be expected that the dehydration of the oxygen vacancy will be independent of the nature of the anion. Likewise, it can be expected that the rehydration of the inserted anion will be directly proportional to their respective dehydration energies and will thus have the effect of reducing the magnitude of the differences between the overall ΔG_{Dehydr}'s of the anions. However, the general relationship shown in Equation (3) and, as long as n > p (that is nett anion dehydration), the trends shown in Fig. 3 can be expected to remain valid; i.e. the ΔG_{Dehydr} term favours pitting by the larger halide anions at all temperatures.

3.2 Insertion energy

Although strictly speaking the insertion energy should only contain the electrostatic energy due to inserting a dehydrated anion of radius *r* into an already expanded vacancy, it is easier to also include the electrostatic part of the energy required to expand the oxygen vacancy (not considered earlier by Macdonld[7]) from its initial size to the size at which it is ready to receive the anion, so that the overall process can be written as:

$$V_{O(r_o)}^{\bullet\bullet} + X_{(r)}^- \xrightarrow{\Delta G_{Insert}} X_{O(r_{xo})}^{\bullet} \tag{5}$$

The energy required to place a charge into a dielectric

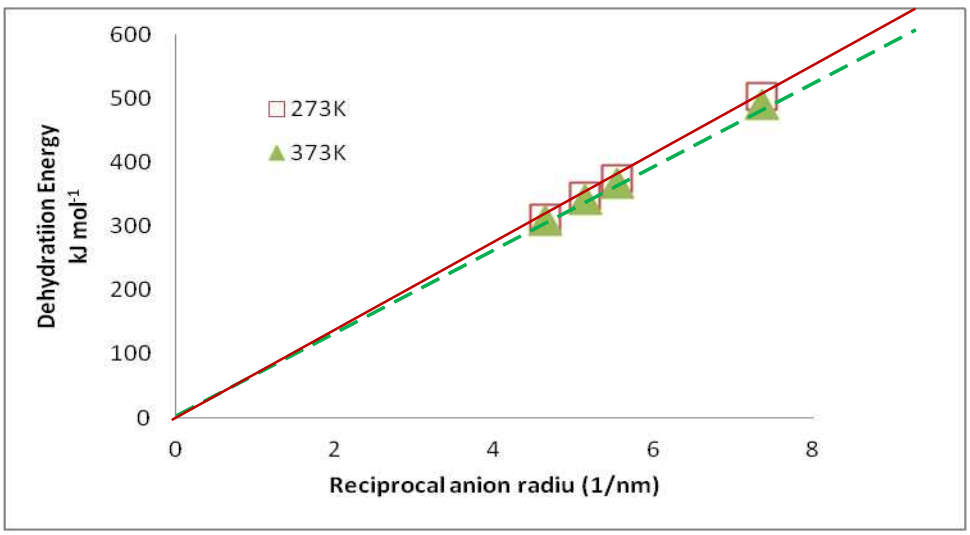

Fig. 3. ΔG_{Dehydr} versus the reciprocal of the anion radius at 273K (brown open squares) and 373K (green triangles).

can be determine from the Born model for electrostatic energy:

$$\Delta G^{\theta}_{solvation} = \frac{N_v Z^2 e^2}{8\pi\varepsilon_0 r}\left(\frac{1}{\varepsilon}-1\right) \quad J\ mol^{-1} \qquad (6)$$

where N_v is Avogadro's number, Ze is the is the magnitude of the charge, ℳ is the dielectric constant of the solvent and ε_0 is the permittivity of free space. Thus the insertion energy to place an ion in to an oxygen vacancy is:

$$\Delta G^{\theta}_{Insert} = \frac{N_v Z^2 e^2}{8\pi\varepsilon_0}\left[\frac{1}{r_{x_0}}\left(\frac{1}{\varepsilon_{ox}}-1\right) - \left(\frac{4}{r_0}\left(\frac{1}{\varepsilon_{ox}}-1\right)+\frac{1}{r}\left(\frac{1}{\varepsilon_{aqu}}-1\right)\right)\right] \quad J\ mol^{-1} \qquad (7)$$

with r_{XO} being approximately equal to whichever is the larger of r_o or r. It can be seen that the middle term in Equation (7) is independent of the size of the anion, depending only on the size of the oxygen vacancy, this term is also found to be dominate having a value close to 2 MJ mol^{-1}. Strictly speaking ΔG_{Insert} should contain two entropy terms due to the changes in the halide concentrations in the solution and in the oxide, however as these will have opposite signs and can be expected to be off similar size they will almost cancel out and have thus be ignored in the present work.

The only parameter in Equation (7) expected to change significantly with temperature is ℳ$_{aqu}$, with values of 88 and 55.3 at 0 ℃ and 100 ℃ respectively[14]; the dielectric constant of transition metal oxides increases by only about 10^{-3} K^{-1} [15,16] and as mentioned above the small coefficient of expansion of oxides means r_o will not change significantly. As a result ΔG_{Insert} is virtually independent of temperature for practical anion sizes. Table 2 shows calculated values for ΔG_{Insert}, at 0 ℃ and 100 ℃, based the r_o and ε_{ox} values of 0.14 nm (radius of O^{2-} ions [12]) and 12 (typical literature value for Cr_2O_3 [17]).

Table 2. Sizes and calculated insertion energies of the various halide ions

Anion	Size (Å)	ΔG (MJ mol^{-1})
F-	1.36	1.844
Cl-	1.81	1.833
Br-	1.95	1.833
I-	2.16	1.831

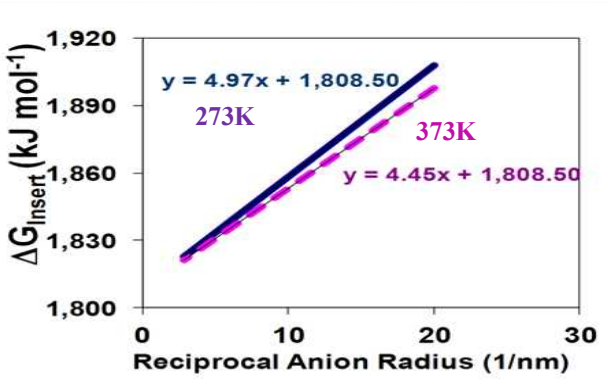

Fig. 4. ΔG_{Insert} versus the reciprocal of the anion radius at 273K (solid line) and 373K (dashed line).

Fig. 4 shows plots of ΔG_{Insert} versus the reciprocal of the anion radius at 273K and 373K, assuming an oxygen vacancy size of 0.14 nm and a value for ε_{ox} of 12, which can be seen to linear. Hence of ΔG_{Insert} can be expressed as a function of temperature and anion radius:

$$\Delta G_{Insert} = \frac{(a'-b'T)}{r} + 1{,}808 \quad kJ\ mol^{-1} \qquad (8)$$

where a' and b' constants. As the derivative of ΔG_{Insert} with respect to temperature is expected to be negative, increasing the temperature will make pitting more favourable but there should be no change in the order of aggressiveness of the ions.

Unfortunately the values in Table 2 (although similar to the values estimated by Macdonald[7]) are unrealistically large for a chemical reaction, being dominated by the loss of the doubly charged oxygen vacancy. In contrast Girault[18] has shown reviewed the electrostatic energy involved in the transfer of ions between two immiscible liquids and for the case where the ionic centre is located on the boundary between the two dielectic liquids (equivalent to adsorption onto a solid surface) this is given by (at other locations complications arise from the need to consider interaction of the ion with its image):

$$\Delta G^{\theta}_{electrostatic} = \frac{N_v Z^2 e^2}{\varepsilon_0(\varepsilon_1+\varepsilon_2)r} \quad J\ mol^{-1} \qquad (9)$$

For a 0.2 nm anion between an aqueous solution and a liquid with a dielectic constant of 12 this yields a value for the insertion energy of 87 kJ mol^{-1} at 0 ºC. It is thus believed that Equation (8) likely vastly over estimates ΔG_{Insert}, nevertheless since Equations (6) and (9) have the

same form it is expected that the following general expression remains value.

$$\Delta G_{Insert} = \frac{(a' - b'T)}{r} + \text{Constant} \quad kJ\ mol^{-1} \qquad (10)$$

3.3 Expansion energy

The energy required increase the physical size of the oxygen vacancy to a size that is sufficiently large to allow the anion to be inserted into it can be derived from basic thermodynamics with Macdonald showing this to be[7] :

$$\Delta G^{\vartheta}_{Exp,Phys} = \Delta H^{\vartheta}_{Exp} - T\Delta S^{\vartheta}_{Exp}$$

$$, = \Delta U^{\vartheta}_{Exp} + P\Delta V - T\Delta S^{\vartheta}_{Exp}$$

$$\approx \frac{4\pi N_v T}{3}\left(\frac{\alpha}{\beta}\right)\left(r^3 - r_0^3\right) - 3RT\,Ln\left(\frac{r}{r_0}\right) \qquad (11)$$

Where ΔU is the change in internal energy, α and β are the coefficients of thermal expansion and compressibility of the passive film. It can be seen that the first (internal energy) term increases with the magnitude of r_{xo} and thus favours pitting by smaller anions, whereas the second (entropy) term decreases and thus favours pitting by larger ions. Therefore plots of $\Delta G_{Exp,phys}$ against anion radius display a minimum, the value of which depends on the size of the initial oxygen vacancy. Macdonald has argued that this could explain why the relative aggressiveness of the halides varies with the nature of the passive film[7].

However, the minimum in $\Delta G_{Exp,phys}$ cannot explain the influence of temperature on the relative aggressiveness of the various halide ions, since Equation (11) can be rearranged to:

$$\frac{\Delta G^{\vartheta}_{Exp,Phys}}{T} = \frac{4\pi N_v}{3}\left(\frac{\alpha}{\beta}\right)\left(r^3 - r_0^3\right) - 3R\,Ln\left(\frac{r}{r_0}\right) \qquad (12)$$

so assuming that α and β are effectively independent of temperature, which should be valid for the relatively small temperature range presently investigated (< 100 degrees centigrade), for any given oxygen vacancy size the minimum in the $\Delta G_{Exp,phys}$ versus r_x curve will be independent of temperature and always very close to the chosen r_o value (Fig. 5); i.e. this cannot explain the cross

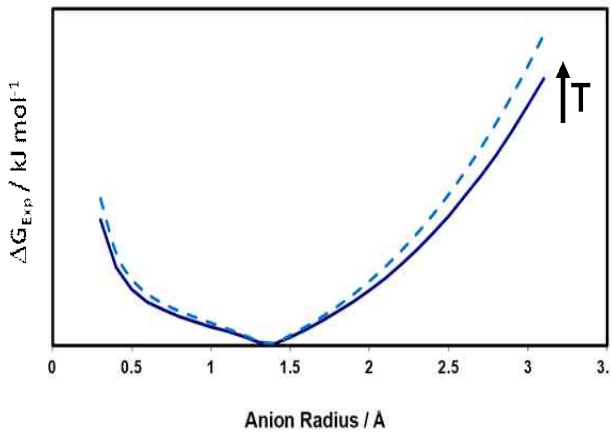

Fig. 5. Illustration of how increasing the temperature (solid to dashed lines) does not shift the minimum in the ΔG_{Dehydr} versus anion radius plot.

over in aggressiveness with increasing temperature seen between chloride and bromide (Fig. 2). Furthermore, Equation (12) also reveals that $\Delta G_{Exp,phys}$ will increase with increasing temperature, meaning that this energy term favours pitting at lower temperatures, i.e. the opposite to well established fact. Of course the observation that ΔG_{Dehydr} and ΔG_{Insert} which decrease with increasing temperature could more than compensate for the increase in the $\Delta G_{Exp,phys}$ term.

3.4 Total energy

To explain the influence of temperature on the order of the relative aggressiveness of the various halides all three energy terms need to be considered, which from Equations (3), (8) and (11) can be written as:

$$\Delta G_{Tot} = \Delta G_{Dehydr} + \Delta G_{Insert} + \Delta G_{EXP}$$

$$\Delta G_{Tot} = \frac{(a - bT)}{r} + \frac{(a' - b'T)}{r} + 1{,}808 +$$

$$\frac{4\pi N_v T}{3}\left(\frac{\alpha}{\beta}\right)\left(r^3 - r_0^3\right) - 3RT\,Ln\left(\frac{r}{r_0}\right) \quad kJ\ mol^{-1} \qquad (12)$$

Neglecting the final entropy term (in practice $r < 1.5\ r_o$ so this term always less than 4 kJ mol^{-1}) and differentiating with respect to r leads to:

$$\frac{\partial\left(\Delta G_{Tot}\right)}{\partial T} = 4\pi N_v T\left(\frac{\alpha}{\beta}\right)r^2 - \frac{(a'' - b''T)}{r^2} \qquad (13)$$

where a" and b" are again constants. The optimum radi-

us, r_{opt}, for pitting can be found by minimizing Equation (13):

$$r_{opt} = \left(\frac{(a''-b''T)}{4\pi N_v T\alpha} \beta \right)^{\frac{1}{4}} \quad (14)$$

As long as a″ is larger than b″T Equation (14) will yield a real number and thus an optimum radius for pitting will exist.

The temperature dependence of r_{opt} can now be found by differentiating with respect to temperature:

$$\frac{\partial r_{opt}}{\partial T} = -\frac{a''\beta}{16\pi N_v \alpha T^2} \left(\frac{(a''-b''T)}{4\pi N_v T\alpha} \beta \right)^{-\frac{3}{4}} \quad (15)$$

The fact that $\frac{\partial r_{opt}}{\partial T}$ is negative means that an increase in temperature will favour pitting by smaller anions, i.e. it agrees with the experimental observation that chloride becomes more aggressive than bromide at higher temperatures. Fig. 6 graphically conveys the same argument that the intercept of the energies that favour pitting by larger anions and the expansion energy term that favours smaller anions will shift to the left as the temperature increase (decreasing r_{opt}). Qualitatively this suggests that at low temperatures both Br^- and Cl^- are smaller than the optimum size, so ΔG_{Dehyd} dominates and Br^- is the more aggressive, while at high temperature Br- becomes larger than the r_{opt} so ΔG_{Exp} dominates and Cl^- is the more aggressive. The I^- ions are presumably always larger than the optimum size so these are the least aggressive of the halide ions investigated at all temperatures studied.

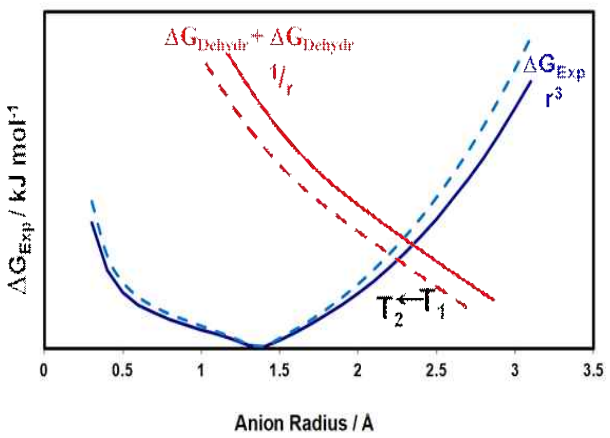

Fig. 6. Graphical depiction of how the minimum in the total adsorption energy (intercept of the red and blue curves) shifts to smaller anion radii as the temperature increases (solid to dashed curves) indicating a decrease in r_{opt}.

However, although the point defect model appears to be able to qualitatively explain the influence of anion size on the pitting potential along with how the relative aggressiveness of different sized anions vary in response to a change in temperature, an attempt at a quantitative fit raises a number of issues. The most important of which is small magnitude of the $\Delta G_{Exp.}$, which is the only term that favours pitting by smaller anions. When typical values for α (7.3×10^{-6} K^{-1}; Cr_2O_3[16]) and β (4.6×10^{-7} atm^{-1}; for TiO_2 rutile as no values for reliable iron or chromium oxides are available[19]) are used along with the anion radii in Table 1 and an estimate for r_o of 0.14 nm (radius of O^{2-} ions) it is found that never $\Delta G_{Exp.phys}$ exceeds 10 kJ mol^{-1} for any halide ion at 353K and its value for chloride ions changes by only 1.0 kJ mol^{-1} over the temperature range studied; equivalent to only 10 mV for a one electron process. This is too small to account for the variation in relative aggressiveness of the halide ions with temperature. Nevertheless, the mechanical properties of the thin oxide films are likely to be considerably different to their bulk counterparts, although it would required the coefficient of compressibility of the thin film to be about two orders of magnitude smaller to produce $\Delta G_{Exp.phys}$ values that could reasonably explain the observed pitting behaviour.

4. Conclusions

By analysing how temperature will influence the energetics of the adsorption of an aggressive ion into a surface oxygen vacancy it has been possible to show that the point defect model can qualitatively explain why the order of aggressiveness of halide ions to stainless steels changes from $Br^- > Cl^- > I^-$ at low temperature to $Cl^- > Br^- > I^-$ at high temperatures. However, unless the mechanical properties of the thin passive oxide films are drastically different from their bulk counterparts the point defect model fails at the quantitative level.

Acknowledgments

This research is supported by the Agency for Science, Technology & Research (A*STAR) under Project No. 112 300 4013.

References

1. D. J. Blackwood, and S. E. Chua, *Proceedings of the 17th International Corrosion Congress on Comparison on in-*

fluence of molybdenum on the pitting of stainless steels in chloride and bromide solutions, p. 72, Perth, Australia (2011).
2. A. I. Munoz, J. G. Anton, J. L. Guinon and V. P. Herranz, *Corros. Sci.*, **48**, 3349 (2006).
3. J. E. Truman, Stainless steels, Corrosion 3rd ed., (eds. L. L. Shrier, R. A. Jarman and G. T. Burstein), Vol. 1, Chapter 3, p. 34, Butterworth-Heinemann, Oxford (1994).
4. G. S. Frankel, *J. Electrochem. Soc.*, **145**, 2186 (1998).
5. J. R. Galvele, *J. Electrochem. Soc.*, **123**, 464 (1976).
6. P. C. Pistorius and G. T. Burstein, *Phil. Trans. R. Soc. A*, **341**, 531 (1992).
7. D. D. Macdonald, *Proceedings of the Electrochemical Society on Pits and pores II : Formation, properties, and significance for Advanced Materials,* **2000-25**, 141, Phoenix, Arizona (2000).
8. D. D. Macdonald, *Corros. Eng. Sci. Techn.*, **49**, 143 (2014).
9. ASTM G-61-86: Standard test method for conducting cyclic potentiodynamic polarization measurements for localized corrosion susceptibility of iron-, nickel-, or cobalt-based alloys, ASTM International, West Conshohocken, PA, USA Re-approved (2009).
10. R. T. DeHoff, Thermodynamics in materials science, p. 409, McGraw Hill Inc., Singapore (1993).
11. R. Schmid, A. M. Miah, and V. N. Sapunov, *Phys. Chem. Chem. Phys.*, **2**, 97 (2000).
12. B. E. Conway and E. Aryranci, *J. Solution Chem.*, **28**, 163 (1999).
13. J. L. Trompette, *Corros. Sci.*, **82**, 108 (2014).
14. C. G. Malmberg and A. A. Maryott, *J. Res. Nat. Bur. Stand.*, **56**, 2641 (1956).
15. K. V. Rao, A. Smakula, *J. Appl. Phys.*, **36**, 2031 (1965).
16. K. Taneichi, T. Narushima, Y. Iguchi and C. Ouchi, *Mater. Trans.*, **47**, 2540 (2006).
17. P. H. Fang and W. S. Brower, *Phys. Rev.*, **129**, 1561 (1963).
18. H. H. Girault, Charge transfer across liquid-liquid interfaces, *Modern Aspects of Electrochemistry*, **25**, p. 1, Plenum Press, New York (1993).
19. C. E. Weir, *J. Res. Nat. Bur. Stand.*, **69A**, 29 (1965).